Three-dimensional analysis of rodent paranasal sinus cavities from X-ray computed tomography (CT) scans

Jonathan E. Phillips, Lunan Ji, Maria A. Rivelli, Richard W. Chapman, Michel R. Corboz

Abstract

Continuous isometric microfocal X-ray computed tomography (CT) scans were acquired from an AKR/J mouse, Brown-Norway rat, and Hartley guinea pig. The anatomy and volume of the paranasal sinus cavities were defined from 2-dimensional (2-D) and 3-dimensional (3-D) CT images. Realistic 3-D images were reconstructed and used to determine the anterior maxillary, posterior maxillary, and ethmoid sinus cavity airspace volumes (mouse: 0.6, 0.7, and 0.7 mm^3, rat: 8.6, 7.7, and 7.0 mm^3, guinea pig: 63.5, 46.6 mm^3, and no ethmoid cavity, respectively). The mouse paranasal sinus cavities are similar to the corresponding rat cavities, with a reduction in size, while the corresponding maxillary sinus cavities in the guinea pig are different in size, location, and architecture. Also, the ethmoid sinus cavity is connected by a common drainage pathway to the posterior maxillary sinus in mouse and rat while a similar ethmoid sinus was not present in the guinea pig. We conclude that paranasal sinus cavity airspace opacity (2-D) or volume (3-D) determined by micro-CT scanning may be used to conduct longitudinal studies on the patency of the maxillary sinus cavities of rodents. This represents a potentially useful endpoint for developing and testing drugs in a small animal model of sinusitis.

Résumé

Des images par tomodensitométrie (CT) isométrique microfocale en continu ont été obtenues de souris AKR/J, de rat Brown-Norway et de cobaye Hartley. L'anatomie et le volume des cavités des sinus paranasaux ont été définis à partir d'images CT en deux dimensions (2-D) et en trois dimensions (3-D). Des images 3-D réalistes ont été reconstruites et utilisées pour déterminer les volumes d'espace d'air des sinus maxillaire antérieur, maxillaire postérieur et ethmoïde (souris : 0,6, 0,7 et 0,7 mm^3; rat : 8,6, 7,7 et 7,0 mm^3; cobaye : 63,5, 46,6 mm^3, et pas de cavité ethmoïde). Les cavités des sinus paranasaux de la souris sont similaires aux cavités correspondantes du rat, avec une réduction de la taille, alors que chez le cobaye les cavités des sinus maxillaires correspondants sont différentes en taille, localisation et architecture. Également, chez la souris et le rat la cavité du sinus ethmoïde est connectée par une voie commune de drainage au sinus maxillaire postérieur alors que chez le cobaye un sinus ethmoïde similaire n'était pas présent. Nous avons conclu que l'opacité de l'espace d'air de la cavité sinusale (2-D) ou le volume (3-D) déterminés par micro-CT pourraient être utilisés pour effectuer des études longitudinales sur la perméabilité des cavités des sinus maxillaires des rongeurs. Ceci représente un critère d'évaluation potentiellement utile pour développer et tester des médicaments dans un modèle de sinusite chez un petit animal.

(Traduit par Docteur Serge Messier)

Introduction

Sinusitis is an extremely common and painful disease that originates from a body cavity with no confirmed function. The human paranasal sinuses are located in the front of the face in the forehead (frontal sinuses), between the eyes (ethmoid and sphenoid sinuses), and in the cheekbones (maxillary sinuses). Each sinus is lined with ciliated epithelium and is directly connected to the nasal cavity through a series of openings in the lateral nasal wall. Some postulated functions of the sinuses are to humidify inspired air, supply resonance to the voice, regulate intranasal pressure, insulate from heat loss, aid in olfaction, and lighten the skull (1–3). Sinusitis is defined as inflammation of one or more of the paranasal sinuses, with the maxillary sinuses frequently being affected (1). Although sinusitis and rhinitis are commonly combined under the term rhinosinusitis, as rhinitis typically precedes sinusitis and sinusitis without rhinitis is rare (4,5); sinusitis has recently been designated as a distinct disease entity by the US Food and Drug Administration (FDA) due to its differences in pathophysiology and treatment from rhinitis (6).

The sinuses are the major air-filled cavities of the skull and air space within these cavities is their most important anatomical feature. Obstruction of the paranasal sinus openings or ostia, as a consequence of viral infection followed sometimes by a secondary bacterial (7) or fungal (8) infection of the sinuses, appears to be a crucial factor in the development of sinusitis (9,10). Therefore the gas-filled volume in the sinuses is the most important index used in the evaluation of the sinuses (11) and computed tomography

Pulmonary and Peripheral Neurobiology, Schering-Plough Research Institute, 2015 Galloping Hill Road, Kenilworth, New Jersey 07033, USA.

Address all correspondence to Dr. Jonathan E. Phillips; telephone: (908) 704-5532; fax: (908) 740-7175; e-mail: jonathan.phillips@spcorp.com

A preliminary report of this work was given at the 2007 American Thoracic Society International Conference on May 19 in San Francisco, California, USA and published in abstract form (Am J Respir Crit Care Med 175:A671).

Received February 4, 2008. Accepted July 21, 2008.

(CT) scanning plays an important role in diagnosis of sinusitis (12). Computed tomography scanning is the primary screening method for pathological conditions of the sinus cavities (13), as mucosal thickening and mucin accumulation create areas of high attenuation on the CT images (opacity) (14). The ability of CT images to optimally display bone, soft tissue/fluid, and air density differences facilitates an accurate depiction of anatomy, and also can be used to monitor the extent of disease progression/remission in and around the paranasal sinuses over time.

There are limitations in the types of studies that can be performed on human subjects. Information obtained from nasal secretion, nasal mucosa, nasal polyps, sinus secretion, and sinus mucosa are not fully satisfactory. Therefore, development of a preclinical animal model of sinusitis is absolutely necessary to overcome the limitations imposed on the study of human subjects and will also advance the development of novel drug products for sinusitis. However, little is known about the paranasal sinuses in small animals. Unlike humans (2), the maxillary sinuses in rodents are not completely enclosed by the upper jaw bone (maxilla). For this reason, maxillary sinuses in rodent and many nonhuman animals are often referred to as maxillary recesses in the literature (15,16). The visualization and measurement of the small rodent paranasal sinuses is difficult.

In the present study, the nasal compartment of 3 different species (mouse, rat, and guinea pig) is evaluated by using microfocal X-ray computed tomography (micro-CT) to determine the volume of the maxillary sinus and to identify the most appropriate small animal sinusitis research model. Indeed, the rabbit has been used frequently and is very helpful in simulating human disease, but the relative lack of experimental reagents and inability to manipulate these animals genetically have made the transition to rodent research necessary. Our results show that the mouse paranasal sinus cavities are similar to the corresponding rat cavities, with a reduction in size; while the corresponding maxillary sinus cavities in the guinea pig are different in size, location, and architecture. We conclude that micro-CT is a valid method for assessment of the maxillary sinus volume in rodents and may be a valuable diagnostic tool in defining disease pathophysiology in rodent models of sinusitis. We recommend the use of the guinea pig as the species for development of a small animal model of sinusitis, due to their epithelial/submucosal structure and larger maxillary sinus cavities.

Materials and methods

Computed tomography scanning

In vivo scans were performed on a female AKR/J mouse (20 g), a male Brown-Norway rat (250 g), and a male Hartley guinea pig (350 g) by anesthetizing the animals with 100 mg of ketamine per kg body weight (BW). These experiments were performed with the prior approval of the Animal Care and Use Committee of Schering-Plough Research Institute. All studies using animals were done in accordance with the National Institutes of Health Guide for the Care and Use of Laboratory Animals and the Animal Welfare Act in a program approved by the Association for Assessment and Accreditation of Laboratory Animal Care International. Computed tomography scans of the head were obtained in the coronal plane [StraTec Medizintechnik XCT Research SA+, Pforzheim, Germany (17)] with 330–550 μA and 52kV (peak). Collimations of 0.26 mm (mouse) and 0.46 mm (rat and guinea pig) were used corresponding to slice thicknesses of 200 μm and 1 mm, respectively. The dimensions of the pixels were 70 × 70 μm. Scanning speed was between 3 and 5 min per slice depending on the size of the animal scanned. The opacity of each pixel is represented by a 16-bit gray-scale value. Each 2-D image file consisted of a 503 × 503 (mouse) or 750 × 750 (rat and guinea pig) matrix of pixels after removing the file header.

3-D reconstruction

Slicer open source software (www.slicer.org; The Brigham and Women's Hospital, Boston, Massachusetts, USA) was used to segment and perform 3-D reconstruction of the sinus cavities and skull. Manual segmentation was performed inside the tissue lining of the sinuses. Three-dimensional reconstruction was performed for volumetric analysis and visualization of the sinuses. Automatic segmentation with CT values between 400 and 3200 was used to segment the bone. Head and paranasal sinus 3-D reconstructions were combined to enhance visualization.

It should also be noted that the morphometric micro-CT analysis is not a fully automated procedure. Indeed, micro-CT morphometry still depends on human judgment and the accuracy of the morphometric measurements is restricted to the voxel size that determines resolution. The voxel size in our mouse scans were 0.001 mm^3 and rat/guinea pig scans were 0.005 mm^3, demonstrating that semi-automated micro-CT analysis of the maxillary rodent sinuses is feasible.

Results

The anatomical location and structure of anterior and posterior maxillary sinus cavities (lateral recesses) in a 2-D cross section of the mouse, rat, and guinea pig head are shown in Figure 1 (portion of the anterior maxillary sinus) and Figure 2 (portion of the posterior maxillary sinus). By stacking the consecutive 2-D images, realistic 3-D images could be reconstructed (Figure 3). The paranasal sinus cavities studied in the mouse are analogous to the rat, with a reduction in size, while the guinea pig cavities possess a different architecture and location in the nasal capsule.

The anterior maxillary sinus of the mouse (Figure 1A) and rat (Figure 1B) are formed primarily by the incisive and maxillary bones and located medial to the caudal end of the upper incisor tooth root. The anterior maxillary sinus of the guinea pig (Figure 1C) is formed primarily by the nasal and incisive bones and located superior to the caudal end of the upper incisor tooth root. The posterior recess of the guinea pig anterior maxillary sinus cavity does pneumatize into the maxillary bone (Figure 1C). The medial walls and ostia are formed by naso- and maxillo-turbinates in all species studied. The volume of the right anterior maxillary sinus of the mouse, rat, and guinea pig are 0.6 mm^3, 8.6 mm^3, and 63.5 mm^3, respectively (Figure 3).

The posterior maxillary sinus of the mouse (Figure 2A), rat (Figure 2B), and guinea pig (Figure 2C) are formed primarily by the maxillary bone. In the rat and guinea pig, but not the mouse due to the inferior position within the nasal capsule, the anterior portion

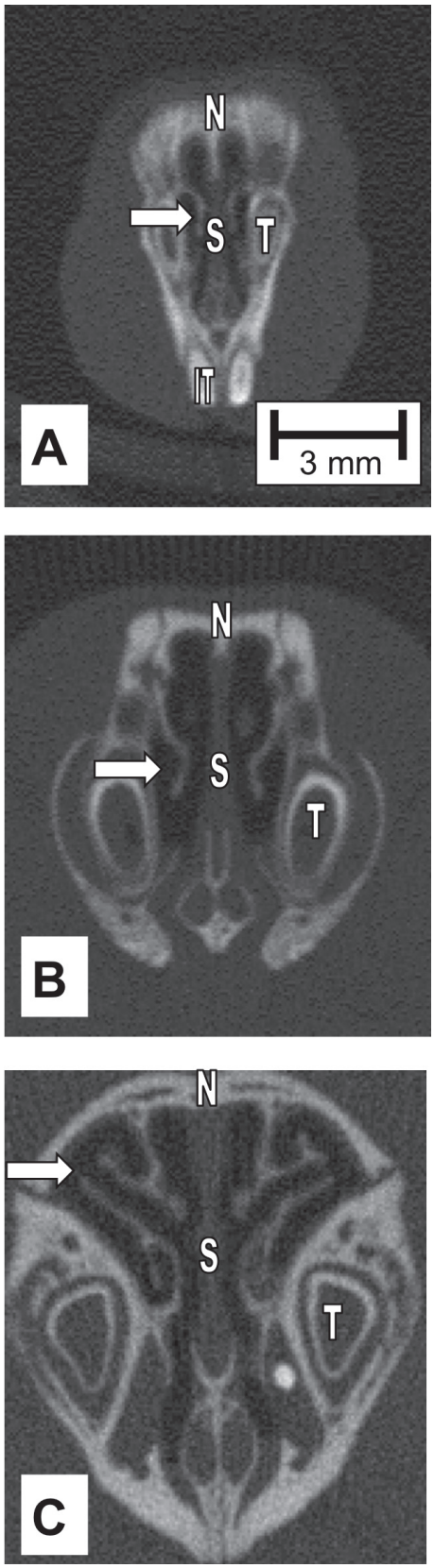

Figure 1. Mouse (A), rat (B), and guinea pig (C) head X-ray computed tomography (CT) cross-sectional scans in the coronal plane. Arrows indicate the right anterior maxillary sinus cavity located superior and medial to the root of upper incisor tooth. All scans have the same scale. T = superior tooth, S = septum, N = bridge of nose, IT = inferior tooth.

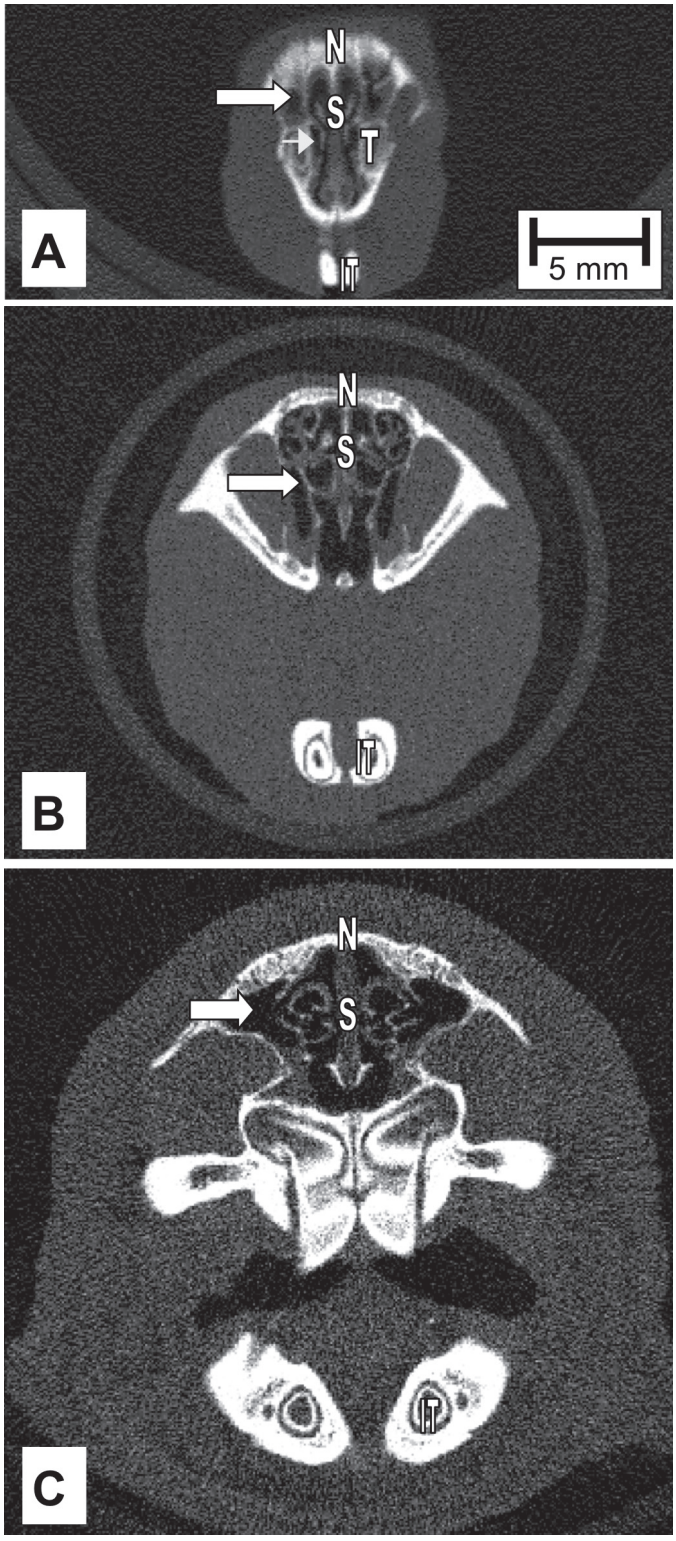

Figure 2. Mouse (A), rat (B), and guinea pig (C) head X-ray computed tomography (CT) cross-sectional scans in the coronal plane. Arrows indicate the right posterior maxillary sinus cavity. Arrowhead in (A) points to anterior maxillary sinus. All scans have the same scale. T = superior tooth, S = septum, N = bridge of nose, IT = inferior tooth.

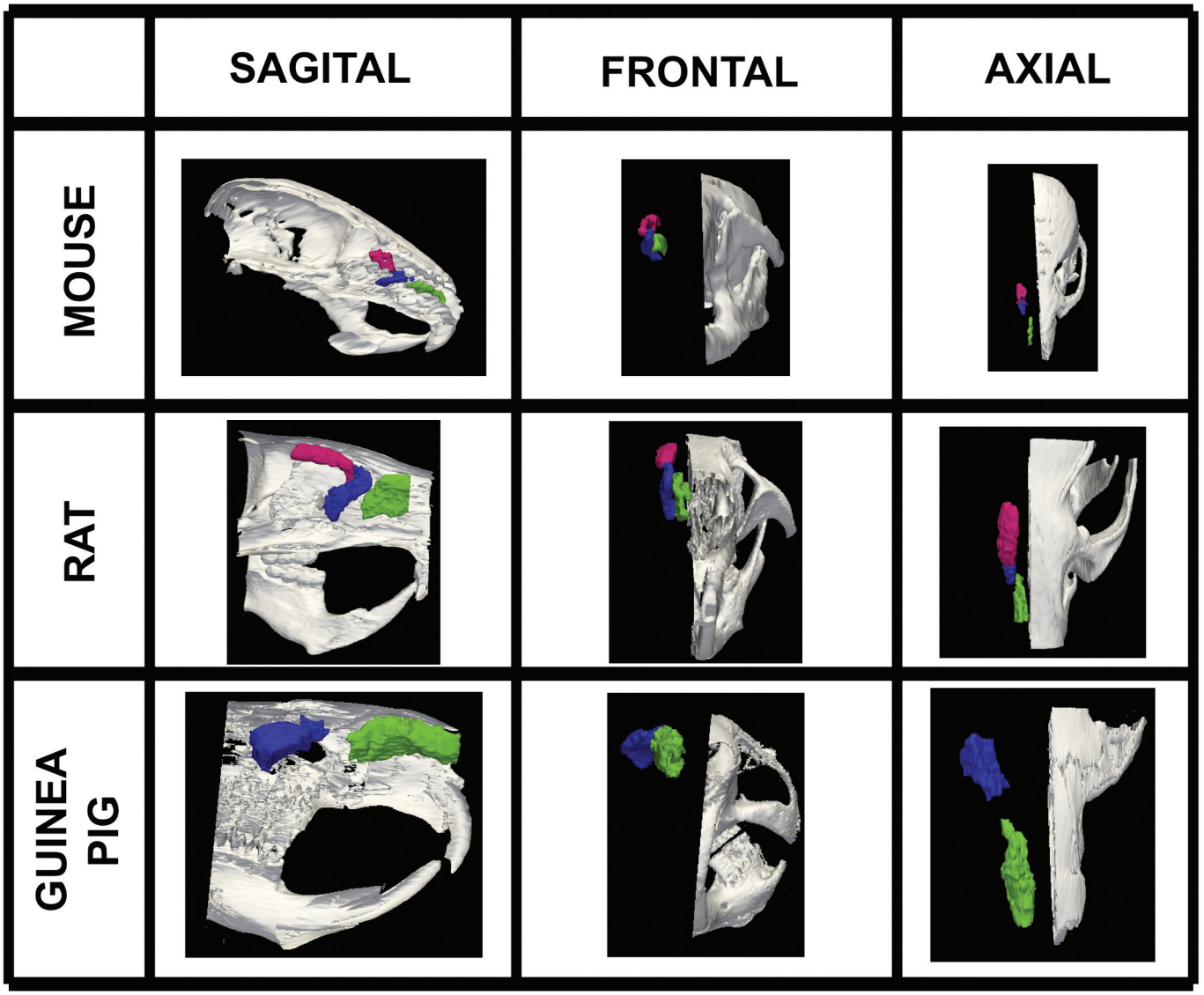

Figure 3. Volumetric surface renderings of paranasal sinus created from sequential computed tomography (CT) images. Three different orientations of the paranasal sinuses (anterior maxillary in green, posterior maxillary in blue, and anterior ethmoid in red) are shown with respect to location in skull according to species, all at different magnifications.

of the posterior maxillary sinus is formed by the nasal and incisive bones. However, the posterior recess of the posterior maxillary sinus cavity in the guinea pig is formed by the frontal bone at the posterior extremity of the nasal capsule (Figure 2C). The anterior portion of the mouse and rat posterior maxillary sinus is located superior to the caudal end of the upper incisor tooth root (Figure 2A and 2B). Conversely, the guinea pig posterior maxillary sinus appears further back in the head, above the molar teeth. The volume of the right posterior maxillary sinus of the mouse, rat, and guinea pig are 0.7 mm^3, 7.7 mm^3, and 46.6 mm^3; respectively (Figure 3).

An ethmoid sinus cavity, defined by endo- and ecto-ethmoturbinates, forms superior to the posterior maxillary sinus and shares a common drainage pathway through the posterior maxillary sinus of the mouse (Figure 4A) and rat (Figure 4B). The guinea pig does not have an ethmoid sinus cavity. The right ethmoid sinus of the mouse and rat are 0.7 mm^3 and 7.0 mm^3, respectively (Figure 4).

Discussion

This study defines the anatomy and represents the first measurements of mouse, rat, and guinea pig maxillary sinus cavity volumes using CT images. The guinea pig posterior maxillary sinus, the most voluminous (46.6 mm^3) among the 3 species, appears further back in the nasal capsule than the corresponding mouse and rat sinus cavities. Mouse and rat ethmoid sinus cavities volumes were 0.7 mm^3 and 7.0 mm^3, respectively; whereas an ethmoid sinus cavity was not present in the guinea pig. We demonstrated that micro-CT scanning offers the sensitivity to assess small animal paranasal sinuses in a noninvasive manner from continuous digital images generated for 2-D or 3-D investigation. The intent of this study was to provide a validation of the micro-CT technique, and a first approximation of its benefits as a research tool. Due to small sample size, the data does not allow for any analysis of individual or intraspecific variation

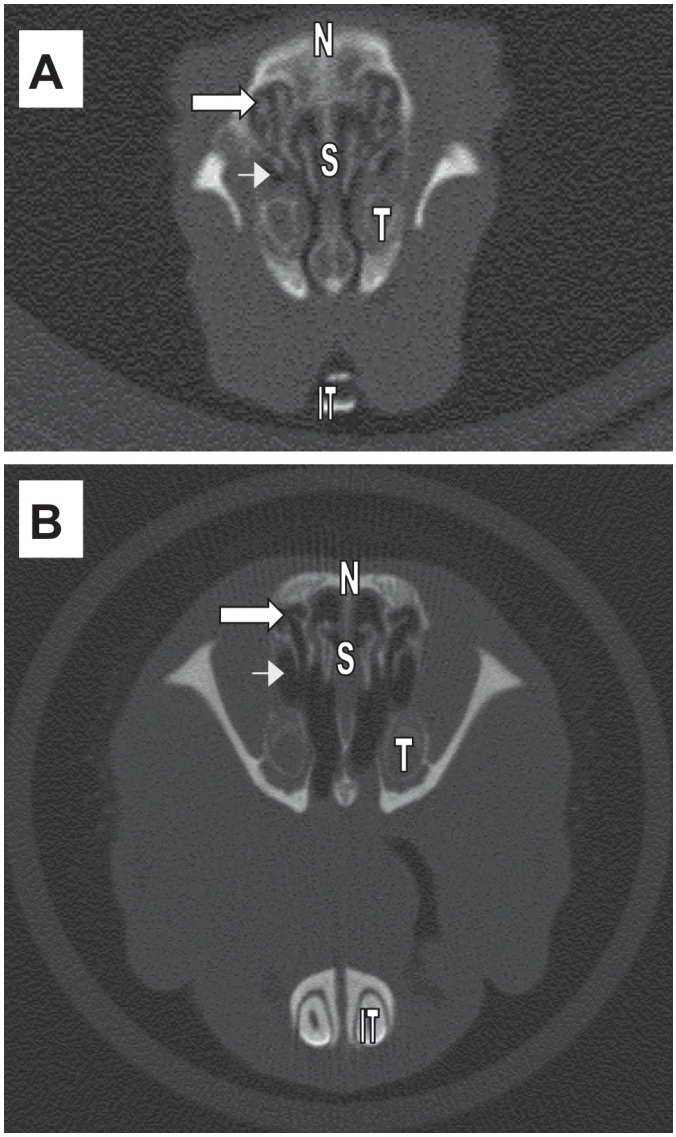

Figure 4. Mouse (A) and rat (B) head X-ray computed tomography (CT) cross-sectional scans in the coronal plane. Arrows indicate the anterior ethmoid sinuses with common drainage pathway into posterior maxillary sinus cavity (arrowhead). Scans do not have the same scale. T = superior tooth, S = septum, N = bridge of nose, IT = inferior tooth.

in cavity size, which varies with ontogenetic age and sex of each individual.

Despite widespread occurrence of sinusitis, the literature lacks information on experimental studies in small animals. Small animals are ideal for drug discovery as their low body mass decreases the amount of drug necessary for conducting preclinical research studies. Recently, the rodent anterior maxillary (18), posterior maxillary (19), and ethmoid (20) sinuses have all been used as models for sinusitis. Bacteria (18,20,21), virus (22), fungus (23), and antigen (19,24) instillation into the sinus cavities; or systemic administration of the nasal toxicant 3-methylindole (25) have all been used to induce sinusitis in rodents. Many of these sinusitis models show histological evidence of luminal or submucosal inflammatory infiltrates (18,22,25,26) that would correlate with the entrapment of thick secretions. These secretions would appear as opacification in the sinuses upon CT imaging. To our knowledge, no rodent sinusitis studies use CT-scans to monitor disease progression and no sinusitis studies in guinea pigs have been reported.

The cavities we refer to as the anterior and posterior maxillary sinuses in the present study have been identified previously in the mouse (27), rat (28), and guinea pig (29). What we refer to as the anterior maxillary sinus has also been referred to as the secondary maxillary sinus (27) and the anterior lateral recess (29) in the literature. What we refer to as the posterior maxillary sinus cavity herein, has been reported previously as the true maxillary sinus (27), posterior lateral recess (29), and maxillary recess (30,31). However, none of the rodent cavities are completely enclosed by bone and are technically not true sinus cavities (15,16), as opposed to the human maxillary sinus which is completely enclosed by a single bone (maxilla) (2). Throughout this manuscript, we refer to the rodent paranasal cavities as "sinus" cavities as it is consistent with current publications, but in the past the rodent paranasal cavities were referred to as "recesses".

A comparison of the anatomy of the posterior maxillary sinus among the species studied revealed that the mouse (27) and rat (present study), but not the guinea pig, have an ethmoid sinus with a common drainage pathway through the posterior maxillary sinus (Figure 4). Jacob and Chole (27) have previously subdivided the mouse ethmoid sinus cavity, as defined in Figure 3 herein, into anterior and posterior portions. The rat posterior maxillary sinus has been previously described (32) as ovoid in shape with supero-inferior and antero-posterior diameters of 4.5 and 9 mm, respectively. Our data are in good agreement with the supero-inferior diameter (Figure 2B) but our antero-posterior measurement is greater (22 mm), possibly because we do not subdivide the ethmoid sinus into anterior and posterior cavities. The measured volume of the posterior maxillary sinus in the present study represents a small part of the total nasal cavity volume (33) of the rat (400 mm^3) and of the total nasal cavity volume of the guinea pig (880 mm^3).

Our data and analysis of the literature suggest the most appropriate rodent model of sinusitis may be a guinea pig posterior maxillary sinus model, although the classification of guinea pigs as rodents is controversial (34). The guinea pig posterior maxillary sinus cavity occupies a large percentage (10.6%) of the total nasal cavity volume versus the rat (3.9%) and mouse (3.5%). By comparison, the human has very large maxillary sinuses, occupying an estimated 60% of the nasal cavity volume, with their entire mucus drainage towards the nasopharynx (35). Rodents have been previously characterized as having small maxillary sinuses (2) with the mucus from the anterior maxillary sinus draining toward the anterior nares and with the mucus from the posterior maxillary sinus draining towards the nasopharynx (35). Also, the submucosa of the mouse and rat posterior maxillary sinus is more densely populated by submucosal glands than their anterior maxillary sinus (21), while both rat and mouse maxillary sinus cavities are lined with respiratory epithelium containing few or no goblet cells (21,32,36–38). In contrast, the submucosa of the guinea pig anterior and posterior maxillary sinus cavities are much less glandular (39) and contain abundant epithelial goblet cells (40), similar to the human maxillary sinus.

Volume of air cavity is the most important index (11) to evaluate the pathophysiology of the paranasal sinuses and we have

demonstrated in this study that the rodent maxillary sinus cavity volume can be determined by using micro-CT. Animal models of sinusitis currently use endpoints like bacteria in nasal lavage, cellular histomorphology (neutrophil clusters, goblet cell hyperplasia, and epithelial thickness) to test the efficacy of potential sinusitis drugs like anti-IL5 antibody (19), leukotriene receptor antagonist (41), antibiotic (20), toll-like receptor 4 agonist (42). With the appropriate animal model and micro-CT, the endpoint of sinus cavity airspace opacity (2-D) or volume (3-D) may also be used to determine if a drug can prevent or decrease the recovery time of an inflamed/occluded maxillary sinus cavity. Monitoring sinus occlusion using a noninvasive imaging method like micro-CT makes it feasible to conduct longitudinal studies on the maxillary sinus cavities of rodents.

Acknowledgment

This research was supported by Schering-Plough Research Institute, Kenilworth, New Jersey, USA.

References

1. Wagenmann M, Naclerio R. Anatomic and physiologic considerations in sinusitis. J Allergy Clin Immunol 1992;90:419–423.
2. Negus V. The Comparative Anatomy and Physiology of the Nose and Paranasal Sinuses. Edinburgh: E & S Livingstone, 1958.
3. Blanton PL, Biggs NL. Eighteen hundred years of controversy: The paranasal sinuses. Am J Anat 1969;124:135–148.
4. Lanza DC, Kennedy DW. Adult rhinosinusitis defined. Otolaryngol Head Neck Surg 1997;117:S1–S7.
5. Benninger MS, Ferguson BJ, Hadley JA, et al. Adult chronic rhinosinusitis: Definitions, diagnosis, epidemiology, and pathophysiology. Otolaryngol Head Neck Surg 2003;129:S1–S32.
6. US Food and Drug Administration. Draft guidance for industry. Sinusitis: Designing clinical development programs for nonantimicrobial drugs for treatment. [FDA Web site]. November 2, 2006. Available at: http://www.fda.gov/cder/guidance/7316dft.htm. Last accessed October 15, 2007.
7. Subcommittee on management of sinusitis and committee on quality improvement. Clinical practice guideline: Management of sinusitis. Pediatrics 2001;108:798–808.
8. Ponikau JU, Sherris DA, Weaver A, Kita H. Treatment of chronic rhinosinusitis with intranasal amphotericin B: A randomized, placebo-controlled, double-blind pilot trial. J Allergy Clin Immunol 2005;115:125–131.
9. Poole MD. A focus on acute sinusitis in adults: Changes in disease management. Am J Med 1999;106:38–47.
10. Berger G, Kattan A, Bernheim J, Ophir D, Finkelstein Y. Acute sinusitis: A histopathological and immunohistochemical study. Laryngoscope 2000;110:2089–2094.
11. Kawarai Y, Fukushima K, Ogawa T, et al. Volume quantification of healthy paranasal cavity by three-dimensional CT imaging. Acta Otolaryngol 1999;s540:45–49.
12. Jun BC, Song SW, Park CS, Lee DH, Cho KJ, Cho JH. The analysis of maxillary sinus aeration according to aging process; volume assessment by 3-dimensional reconstruction by high-resolutional CT scanning. Otolaryngol Head Neck Surg 2005;132:429–434.
13. Mafee M, Tran B, Chapa A. Imaging of rhinosinusitis and its complications: Plain film, CT, and MRI. Clin Rev Allergy Immunol 2006;30:165–186.
14. Shryock TR, Losonsky JM, Smith WC, et al. Computed axial tomography of the porcine nasal cavity and a morphometric comparison of the nasal turbinates with other visualization techniques. Can J Vet Res 1998;62:287–292.
15. Evans HE. Miller's Anatomy of the Dog. Philadelphia: Saunders, 1993.
16. Norris AM. Diseases of the nose and sinuses. Vet Clin North Am Small Anim Pract 1985;15:865–890.
17. Paulus M, Gleason S, Kennel S, Hunsicker P, Johnson D. High resolution X-ray computed tomography. Neoplasia 2000;2:62–70.
18. Jacob A, Faddis B, Chole R. Chronic bacterial rhinosinusitis: Description of a mouse model. Arch Otolaryngol Head Neck Surg 2001;127:657–664.
19. Hussain I, Randolph D, Brody SL, et al. Induction, distribution and modulation of upper airway allergic inflammation in mice. Clin Exp Allergy 2001;31:1048–1059.
20. Naclerio R, Blair C, Yu X, Won Y-S, Gabr U, Baroody FM. Allergic rhinitis augments the response to a bacterial sinus infection in mice: A review of an animal model. Am J Rhinol 2006;20:524–533.
21. Lindsay R, Slaughter T, Britton-Webb J, et al. Development of a murine model of chronic rhinosinusitis. Otolaryngol Head Neck Surg 2006;134:724–730.
22. Ramadan H, Meek R, Dawson G, Spirou G, Cuff C, Berrebi A. Histologic and immunologic observations of viral-induced rhinosinusitis in the mouse. Am J Rhinol 2002;16:61–67.
23. Rodriguez TE, Falkowski NR, Harkema JR, Huffnagle GB. Analysis of the role of neutrophils in preventing and resolving acute fungal sinusitis. Infect Immun 2007;75:5663–5668.
24. Hussain I, Jain VV, Kitagaki K, Businga TR, O'Shaughnessy P, Kline JN. Modulation of murine allergic rhinosinusitis by CpG oligodeoxynucleotides. Laryngoscope 2002;112:1819–1826.
25. Wiethoff AJ, Harkema JR, Koretsky AP, Brown WE. Identification of mucosal injury in the murine nasal airways by magnetic resonance imaging: Site-specific lesions induced by 3-methylindole. Toxicol Appl Pharmacol 2001;175:68–75.
26. Blair C, Nelson M, Thompson K, et al. Allergic inflammation enhances bacterial sinusitis in mice. J Allergy Clin Immunol 2001;108:424–429.
27. Jacob A, Chole RA. Survey anatomy of the paranasal sinuses in the normal mouse. Laryngoscope 2006;116:558–563.
28. Kelemen G, Sargent F. Nonexperimental pathologic findings in laboratory rats. Arch Otolaryngol 1946;44:24–42.
29. Kelemen G. Nasal cavity of the guinea pig in experimental work. Arch Otolaryngol 1950;52:579–596.
30. Hebel R, Stromberg M. Anatomy of the Laboratory Rat. Baltimore: Williams and Wilkins, 1976.
31. Cooper G, Schiller A. Anatomy of the Guinea Pig. Cambridge: Harvard Univ Pr, 1975.
32. Vidic B, Greditzer HG. The histochemical and microscopical differentiation of the respiratory glands around the maxillary sinus of the rat. Am J Anat 1971;132:491–514.

33. Schreider JP. Nasal airway anatomy and inhalation deposition in experimental animals and people. In: Reznik G, ed. Nasal Tumors in Animals and Man. Boca Raton, Florida: CRC Pr, 1983:1–26.
34. D'Erchia AM, Gissi C, Pesole G, Saccone C, Arnason U. The guinea-pig is not a rodent. Nature 1996;381:597–600.
35. Lucas AM, Douglas L. Principles underlying ciliary activity in the respiratory tract. II. A comparison of nasal clearance in man, monkey and other mammals. Arch Otolaryngol 1934;20: 518–541.
36. Mery S, Gross E, Joyner D, Godo M, Morgan K. Nasal diagrams: A tool for recording the distribution of nasal lesions in rats and mice. Toxicol Pathol 1994;22:353–372.
37. Young JT. Histopathologic examination of the rat nasal cavity. Fundam Appl Toxicol 1981;1:309–312.
38. Harkema J, Carey S, Wagner J. The nose revisited: A brief review of the comparative structure, function, and toxicologic pathology of the nasal epithelium. Toxicol Pathol 2006;34:252–269.
39. Rohrbach S, Olthoff A, Laskawi R, Giefere B, Gotz W. Botulinum toxin type A induces apoptosis in nasal glands of guinea pigs. Ann Otol Rhinol Laryngol 2001;110:1045–1050.
40. Mogensen C, Tos M. Quantitative histology of the maxillary sinus. Rhinology 1977;15:129–140.
41. Khoury P, Baroody F, Klemens J, Thompson K, Naclerio R. Effect of montelukast on bacterial sinusitis in allergic mice. Ann Allergy Asthma Immunol 2006;97:329–335.
42. Luxameechanporn T, Kirtsreesakul V, Klemens J, Khoury P, Thompson K, Naclerio RM. Evaluation of importance of Toll-like receptor 4 in acute *Streptococcus pneumoniae* sinusitis in mice. Arch Otolaryngol Head Neck Surg 2005;131:1001–1006.